

Original article

Numerical predicting of the effective thermal conductivity of a zeolite adsorption bed for thermal energy saving

Mingyang Gao¹, Ning Zhou¹, Tao Zhang¹, Chuanyong Zhu¹^{*}, Liang Gong¹^{*}

¹College of New Energy, China University of Petroleum (East China), Shandong 266580, P. R. China

Keywords:

Zeolite
adsorption bed
effective thermal conductivity
Lattice Boltzmann method

Cited as:

Gao, M., Zhou, N., Zhang, T., Zhu, C.,
Gong, L. Numerical predicting of the
effective thermal conductivity of a zeolite
adsorption bed for thermal energy saving.
Computational Energy Science, 2024,
1(3): 127-137.
<https://doi.org/10.46690/compes.2024.03.01>

Abstract:

In this study, an innovative Random Particle Packed Adsorption (RPPA) method was proposed to reconstruct the zeolite adsorption bed, restoring the multi-level pore structure within and between zeolite particles through three packing methods: Quartet Structure Generation Set (QSGS), Simple Cubic (SC) and Face-Centered Cubic (FCC). The effective thermal conductivity (ETC) of the zeolite adsorption bed was predicted using the Lattice Boltzmann Method (LBM) and the results demonstrated a remarkable concordance with experimental values, especially for the SC packing method, with a maximum error of 7.3%. The results show that the QSGS packing method exhibited the highest ETC due to the largest volume fraction of zeolite. Furthermore, the ETC of the adsorption bed increases with increasing water absorption, temperature and zeolite particle contact ratio while decreasing with increasing porosity.

1. Introduction

With the rapid development of modern society and the increasing global energy demand, the transition from traditional fossil fuel-based energy sources to renewable energy sources is a crucial solution to the growing environmental degradation and energy crises (Hua et al., 2022; Li et al., 2022). According to the carbon neutrality targets of major countries in the world, the proportion of renewable energy in the global energy production system will increase from 15% in 2020 to about 56% in 2050. However, renewable energy is characterized by instability and irregularity, resulting in a mismatch between energy supply and demand in terms of time, space and intensity (Marín et al., 2021; Gao et al., 2023). Thermochemical heat storage technology can temporarily store unused or excess heat energy in a specific medium and release it when required, which is the optimal solution for seasonal heat storage (Ristić et al., 2018; Kant and Pitchumani, 2022; Zhu et al., 2024). Moreover, thermochemical storage offers several significant advantages, such as high energy density, low

energy loss and the ability to store energy over the long term (Ye et al., 2022). Consequently, thermochemical heat storage technology presents substantial potential for low-carbon development and sustainable energy use, with extensive applications in heating and cooling scenarios (Gaeini et al., 2018; Zhang and Wang, 2018; Bon et al., 2019). Thermochemical heat storage can be classified into two categories: Thermochemical adsorption heat storage and thermochemical reaction heat storage. Heat is stored in adsorption heat storage by breaking the binding force between the adsorbent and the adsorbate (Kant et al., 2020; Hu et al., 2022).

Porous materials, such as alumina and zeolite, are effective adsorbents used for dehumidification and removing trace gases from the air (Igarashi et al., 1997; Ito, 2000; Li et al., 2022; Lu et al., 2022). When exposed to moist air, these materials undergo physical adsorption, releasing the heat of adsorption (Jänchen et al., 2004; Dicaire and Tezel, 2011; Pérez-Botella et al., 2022). Owing to their high adsorption capacity and stable structural properties, zeolite particles are frequently employed as a preferred medium in the construction of adsorption beds

(Liu et al., 2020; Duan et al., 2023; Madero-Castro et al., 2023; Touloumet et al., 2023; Wijayanta et al., 2023). However, the high porosity of zeolites results in low thermal conductivity (N'Tsoukpoe et al., 2014; Mohammed et al., 2018), which impairs the heat storage performance of the adsorption bed. Therefore, optimizing the heat transfer performance of the adsorption layer is crucial for enhancing the heat transfer efficiency of the adsorption bed and the overall system performance (Dawoud et al., 2011; Rouhani and Bahrami, 2018).

To study and optimize the heat transfer performance of the adsorption bed, the ETC of the adsorption bed needs to be measured and modeled. Existing literature (Rouhani and Bahrami, 2018; Abohamzeh and Frey, 2022) indicates that the ETC of adsorption beds is not a constant value, it is influenced by the components within the adsorption bed and the adsorption environment. Dawoud et al. (2011) employed the transient hot-wire method to determine the effective thermal conductivity of 4A zeolite under various steam pressures, temperatures and water absorption conditions. The values ranged between $0.16 \text{ W}\cdot\text{m}^{-1}\cdot\text{K}^{-1}$ and $0.21 \text{ W}\cdot\text{m}^{-1}\cdot\text{K}^{-1}$. Additionally, Hanif et al. (2019) investigated the effect of relative humidity on the thermal conductivity of zeolite-based adsorbents AQSOA-Z02 and AQSOA-Z05. The experimental results showed an increase in thermal conductivity with higher relative humidity. Although the measurement of the thermal conductivity of the adsorption bed provides the possibility for the real analysis of its thermal performance, it is not economical and feasible to measure the thermal conductivity in a wide range of different experimental environments and particle properties (Sцуiller et al., 2022).

Therefore, it is very important to establish a comprehensive model of the ETC of the adsorption bed for accurate analysis, prediction and improvement of the thermal performance of the adsorption bed (Chen et al., 2022). The initial step involves establishing a model for zeolite adsorption particles, which comprise three components: The zeolite matrix, pore gas and adsorbate. Chu et al. (2020) employed a fractal capillary bundle model to predict the ETC of saturated or unsaturated porous materials, finding that the material's composition significantly influences the ETC due to the differences in thermal conductivity between components. Hence, the thermal conductivity of zeolite adsorption particles is influenced collectively by the zeolite matrix, pore gas and adsorbate. Furthermore, considering the interaction between fluid and solid particles, ETC is regarded as a function of porosity, pore structure of the adsorbent, adsorption capacity and temperature (Tong et al., 2009). Sarwar and Majumdar (1995) studied the effect of humidity on the ETC of particle adsorption beds, observing an increase in gas thermal conductivity with higher humidity. Dawoud et al. (2011) developed a model to calculate the ETC of wetted zeolite 4A. They presumed an isotropic distribution of adsorbed water within the zeolite crystal. The model defined a tortuosity factor for conductive heat transfer and incorporated the Knudsen conductivity of the vapor phase by fitting the experimental data. Rouhani and Bahrami (2018) present a comprehensive model designed to predict the ETC and thermal contact resistance of adsorption beds. The model considers various factors, including water uptake, adsorbent layers, par-

ticle size, bed porosity, temperature, contact pressure and gas pressure across different packing types.

In conclusion, there has been a considerable body of research on predictive models for the ETC of zeolite adsorption beds. Typically, these predictive models couple the thermal conductivity coefficients of the zeolite matrix, pore gas and adsorbate, yielding the theoretical thermal conductivity of solid zeolite adsorption particles. Finally, the ETC for the entire adsorption bed is forecasted by considering the filling structure of zeolite adsorption particles within the bed. However, actual zeolite adsorption particles deviate from the characteristics of solid spherical particles, exhibiting a multi-tiered pore structure that encompasses macro-pores between particles and micro-pores within individual particles. Furthermore, with an increase in adsorption capacity, the outer layers of zeolite adsorption particles become enveloped by the adsorbate, thereby influencing inter-particle contact and substantially affecting the heat conduction process between particles. Consequently, existing models for solid zeolite adsorption particles prove inadequate in accurately capturing these distinctive adsorption characteristics.

This paper introduces a Random Particle Packing Adsorption (RPPA) method based on the Quadruplet Structure Generation Set (QSGS) approach (Wang and Pan, 2007), aimed at describing both the adsorption characteristics and filling structure of adsorption beds. The RPPA method allows for the construction of a porous adsorbent matrix with a specified porosity, generating adsorbates with a given adsorption capacity. This approach provides a more accurate representation of the multi-layered pore structure within the adsorption bed and contributes to a comprehensive description of the adsorption characteristics exhibited by zeolite particles. The Lattice Boltzmann Method (LBM) has been chosen in this study due to its outstanding parallel computing performance and ability to handle complex structures (Guo et al., 2022; Zhu et al., 2022; Lin et al., 2023). Specifically, the D3Q7 model with a multiple-relaxation-time (MRT) collision operator was employed to calculate the ETC of the zeolite adsorption bed. The impacts of adsorption capacity, temperature, porosity and anisotropy degree on the ETC were investigated using three packing methods: QSGS, SC and FCC.

2. Physical problem description and numerical model

2.1 Physical model of three-dimensional zeolite adsorption heat storage adsorption bed

To predict the ETC of a zeolite adsorption bed, a physical model of a three-dimensional porous media adsorption bed was established, as shown in Fig. 1. The model consists of a cube with side length L , including three components: Adsorbent (orange), adsorbate (purple) and pore gas (white), representing the zeolite matrix, adsorbed water and wet air, respectively. The simulation sets the top surface of the adsorption bed as the isothermal thermal boundary, the bottom surface as the isothermal cold boundary and the other four wall surfaces as the adiabatic boundary. Heat flow is transferred

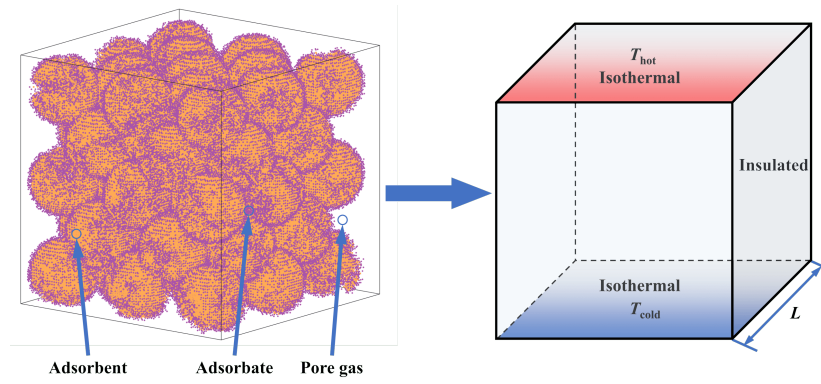


Fig. 1. Three-dimensional adsorption heat storage adsorption bed model and simulated boundary.

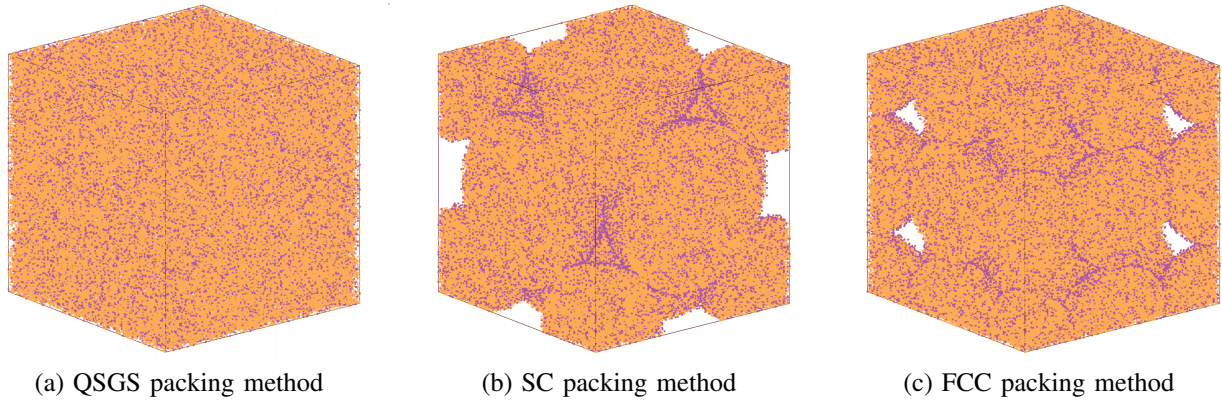


Fig. 2. Adsorption heat storage adsorption bed model with three types of deposition.

through three components: The adsorbent, adsorbate and pore gas, primarily through heat conduction.

2.2 Reconstruction of adsorption heat storage adsorption bed model

Random packing of zeolite particles in the adsorption bed leads to large pores between the particles. Compared to wet air, the thermal conductivity of zeolite is higher ($0.117 \text{ W}\cdot\text{m}^{-1}\cdot\text{k}^{-1}$) (Hanif et al., 2019) and the solid phase volume fraction of the adsorption bed significantly influences the ETC. Simultaneously, during heat release, heated wet air entering the adsorption bed causes water molecules to adsorb into the pores of zeolite particles, increasing the thermal conductivity of the adsorption bed. The RPPA method was used in this study to build three types of adsorption bed models: QSGS, SC and FCC packing methods, as shown in Figs. 2(a), 2(b) and 2(c). The following are the detailed reconstruction steps:

- 1) The zeolite matrix was constructed using the QSGS method. In this step, the main parameters controlling the matrix structure are porosity ε , directional growth probability D_i (i is the growth direction, as shown in Fig. 3, $i=1-26$) and growth nucleus distribution probability c_d . To simplify, the zeolite matrix is assumed to be isotropic, so the probability of directional growth is set to 0.001. At the same time, to achieve a more uniform distribution of the zeolite matrix, the distribution probability of growth

nuclei is set to 0.2. Finally, the zeolite matrix with the given porosity is generated, corresponding to the solid phase volume fraction $\beta_{s,q}$ as follows:

$$\beta_{s,q} = 1 - \varepsilon \quad (1)$$

where the subscript s represents the zeolite matrix and q represents the QSGS method.

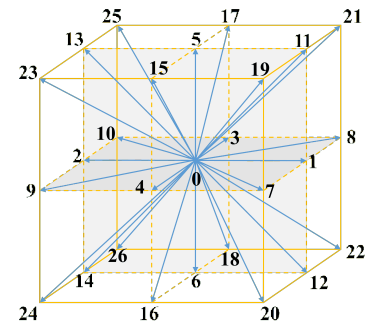


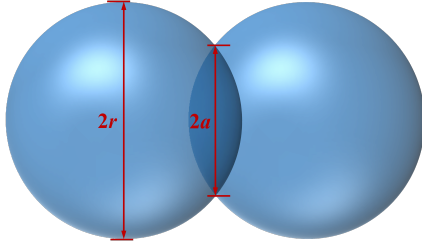
Fig. 3. Schematics of 26 generative directions.

- 2) Spheres were employed to reconstruct zeolite particles using the SC and FCC packing methods. First, the coordinates of the sphere's center were determined and stored for both SC and FCC packing methods. Subsequently, the zeolite matrix coordinates within the sphere radius r were selected and stored, yielding the solid phase volume

Table 1. Specifications of SC and FCC packing methods of an adsorption bed.

Packing arrangement	Bed length	Sphere radius (r)	Boundary cell length (L_b)	Solid phase volume fraction
SC	L	$L/4$	r_{SC}	$\beta_{s,s}$
FCC	L	$L/2\sqrt{2}$	r_{FCC}	$\beta_{s,f}$

fractions $\beta_{s,s}$ and $\beta_{s,f}$ corresponding to the SC and FCC packing methods. The specific parameter settings for this process are detailed in Table 1. It should be noted that, as depicted in Fig. 4, the contact radius between spheres is denoted as a and as the radius of the sphere r increases, the contact ratio of the two spheres a/r increases. Moreover, for random adsorption beds with solid spherical particles, the solid phase volume fraction lies between the SC packing method (0.524) and the FCC packing method (0.74), providing the basis for constructing these two types of adsorption beds in this study (Rouhani and Bahrami, 2018).

**Fig. 4.** Diagram of two contact spheres.

- 3) Utilizing the three types of constructed zeolite substrates as growth nuclei, the adsorbate was generated on the surface of the adsorbent using a simplified QSGS method. The volume fraction of adsorbed water β_w was determined based on water absorption ω , as shown in Eqs. (2) and (3) :

$$\omega = \frac{m_w}{m_s} \quad (2)$$

$$\beta_w = \omega \frac{\rho_s}{\rho_w} \beta_s \quad (3)$$

In the formula, m represents mass, while β_s , ρ_s and ρ_w denote the volume fraction, density and water density of the zeolite matrix, respectively. The subscript w represents adsorbed water. The matrix adsorption using QSGS, SC and FCC packing methods served as growth nuclei to generate adsorbed water, with coordinates saved until the desired water absorption level was achieved. It should be noted that during this process, adsorbed water is assumed to be uniformly distributed. Hence, the directional growth probability is set to 0.001.

2.3 MRT-LBM thermal conductivity model

The thermal conduction equations for an adsorption bed can be expressed as follows:

$$\begin{aligned} (\rho c_p)_s \left(\frac{\partial T}{\partial t} \right) &= k_s \nabla^2 T \\ (\rho c_p)_w \left(\frac{\partial T}{\partial t} \right) &= k_w \nabla^2 T \\ (\rho c_p)_g \left(\frac{\partial T}{\partial t} \right) &= k_g \nabla^2 T \end{aligned} \quad (4)$$

where c_p is the specific heat capacity, k is the thermal conductivity, T is the temperature and t is the time. The subscripts g represent the pore gas.

For heat conduction at different phase interfaces, temperature and heat flux should be continuous:

$$\begin{aligned} T_{a,int} &= T_{b,int} \\ K_a \frac{\partial T}{\partial \mathbf{n}} \Big|_{a,int} &= K_b \frac{\partial T}{\partial \mathbf{n}} \Big|_{b,int} \end{aligned} \quad (5)$$

where “int” represents different phase interfaces, a and b represent the two phases in contact and \mathbf{n} represents the unit normal vector perpendicular to the interface.

In this study, the top and bottom boundaries of the adsorption bed are set as T_h and T_c , respectively, while the side walls are considered to be adiabatic. The ETC of the adsorption bed can be calculated as follows:

$$K_{eff} = \frac{\int q_z dA}{A \Delta T / H} \quad (6)$$

where q_z represents the heat flux passing through the area dA in the z -direction and H is the distance between the top and bottom walls.

The aforementioned equation is solved using the Multiple-Relaxation-Time Lattice Boltzmann method (MRT-LBM) with a dimensional seven-speed (D3Q7) model (Lin et al., 2019; Zhu et al., 2021a). The model demonstrated sufficient accuracy for the heat conduction problem, as well as high numerical stability and computational efficiency (Zhu et al., 2021). The MRT collision operator is shown below:

$$\begin{aligned} f_i(\mathbf{X} + \mathbf{e}_i \Delta t, t + \Delta t) - f_i(\mathbf{X}, t) \\ = -(\mathbf{M}^{-1} \mathbf{S}_g \mathbf{M}) [f_i(\mathbf{X}, t) - f_i^{eq}(\mathbf{X}, t)] \end{aligned} \quad (7)$$

where f_i is the temperature distribution function with $i=0, 1, 2, \dots, 6$; \mathbf{X} represents the location vector; t is the real-time; \mathbf{e}_i is the discrete lattice velocity; f_i^{eq} is the equilibrium distribution function. \mathbf{S}_g and \mathbf{M} are the diagonal relaxation matrix and transformation matrix, respectively. For the D3Q7 model, \mathbf{e} and \mathbf{M} can be given as (Lin et al., 2019):

$$\mathbf{e} = \begin{bmatrix} 0 & c & -c & 0 & 0 & 0 & 0 \\ 0 & 0 & 0 & c & -c & 0 & 0 \\ 0 & 0 & 0 & 0 & 0 & c & -c \end{bmatrix} \quad (8)$$

$$\mathbf{M} = \begin{bmatrix} 1 & 1 & 1 & 1 & 1 & 1 & 1 \\ 0 & 1 & -1 & 0 & 0 & 0 & 0 \\ 0 & 0 & 0 & 1 & -1 & 0 & 0 \\ 0 & 0 & 0 & 0 & 0 & 1 & -1 \\ 0 & 1 & 1 & 1 & 1 & 1 & 1 \\ 0 & 1 & 1 & -1 & -1 & 0 & 0 \\ 0 & 1 & 1 & 0 & 0 & -1 & -1 \end{bmatrix} \quad (9)$$

where $c = \Delta x / \Delta t$, represents the lattice speed and Δx is the lattice size.

For the D3Q7 model, the equilibrium distribution function can be given as:

$$f_i^{eq} = w_i T \quad (10)$$

where w_i is the weight factor, which can be given as:

$$w_i = \begin{cases} 1/4, & i = 0 \\ 1/8, & i = 1 \sim 6 \end{cases} \quad (11)$$

S_g in Eq. 7 can be given as (Lin et al., 2019):

$$\mathbf{S}_g = (S_0, S_1, S_1, S_1, S_2, S_2, S_2) \quad (12)$$

$$S_0 = 0, S_1 = \frac{1}{(D_n/c_s^2/\Delta t + 0.5)}, S_2 = 2 - S_1 \quad (13)$$

where D is the thermal diffusivity and the subscript n can represent s , w or g , $c_s = 0.5$ is the lattice sound speed. The temperature and the heat flux can be calculated by

$$T = \sum_i f_i \quad (14)$$

$$q = \left(\sum_i c_i f_i \right) \frac{1/S_1 - 0.5}{1/S_1} \quad (15)$$

3. Model validation

3.1 Grid independence test

In this study, the porosity of the adsorption bed generated using the QSGS method was set at 0.8. Grid independence validation was performed for the number of grids used in the generated adsorption bed, with the adsorbed water content set to 0 for simplicity. The ambient temperature was set at 25°C, and the thermal conductivity of the zeolite matrix and wet air, which are temperature-dependent functions (Rouhani and Bahrami, 2018), were set at 0.1165 W·m⁻¹·K⁻¹ and 0.0264 W·m⁻¹·K⁻¹, respectively. For the three packing methods, the QSGS packing method with the largest solid phase volume fraction and the packing method with the smallest solid phase volume fraction were selected for verification. As depicted in Fig. 5, the mesh size was varied from 50 × 50 × 50 (a total of 125,000 nodes) to 140 × 140 × 140 (a total of 2,744,000 nodes) to simulate the ETC of the adsorption bed. The predicted value increased with increasing mesh size. For the SC packing method, the ETC tended to stabilize when the mesh size was greater than 90, while for the QSGS packing method, it tended to stabilize when the mesh size was greater

than 70. This finding can be attributed to the difference in the shape of the forming matrix. As a result, in the following study cases of this paper, the mesh size was set to 96 × 96 × 96 (884,736 nodes in total).

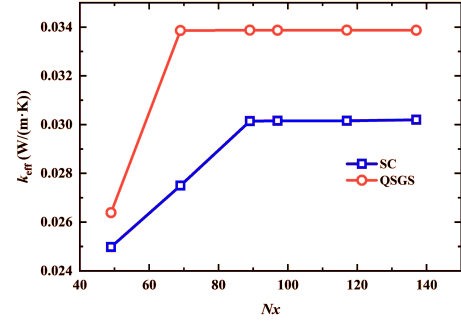


Fig. 5. Effect of mesh size on ETC.

3.2 Series parallel verification of heat conduction

To validate the ETC prediction model, simulations were performed for heat conduction processes in both series and parallel configurations. The computational model employed for validation, depicted in Fig. 6, divides the calculation region into two sections separated by two materials with thermal conductivities k_1 and k_2 , the volume fraction of material 1 is $\beta_1 = 0.7$. The ETC for the series and parallel models can be calculated using the following expressions:

$$\frac{1}{k_{eff}} = \frac{\beta_1}{k_1} + \frac{1 - \beta_1}{k_2} \quad (16)$$

$$k_{eff} = k_1 \beta_1 + k_2 (1 - \beta_1) \quad (17)$$

In the simulations, k_2 is assumed to be 1.0 W·m⁻¹·K⁻¹. Fig. 7 illustrates the comparison between the simulation results and the analytical solutions. The simulation results obtained using the MRT-LBM method show good agreement with the analytical solutions, verifying the reliability of the program.

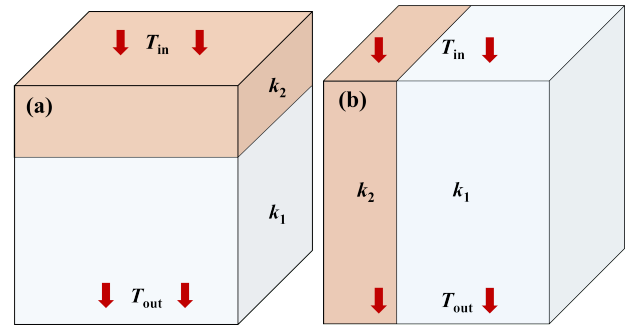


Fig. 6. Two basic heat conduction structures: (a) Series mode; (b) Parallel mode.

3.3 Experimental verification of simulation results

To further validate the accuracy of the simulation results, the calculated results obtained using the SC and FCC packing methods were compared with the experimental results of Hanif et al. (2019). Assuming that the thermal conductivity

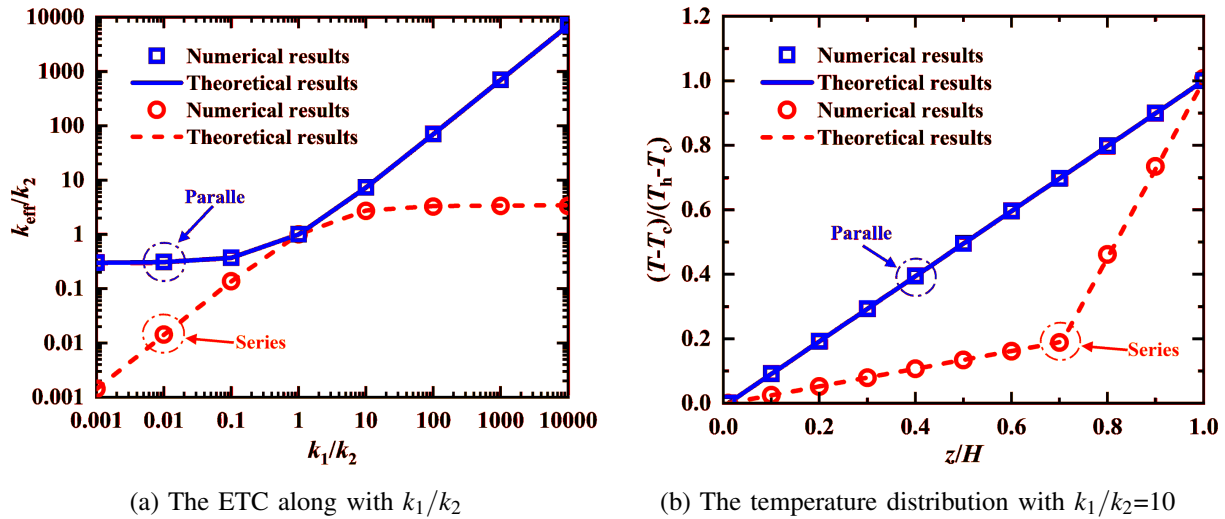


Fig. 7. ETC and temperature distribution of parallel and series models.

of the zeolite adsorbent AQSOA-Z02 at 25 °C is $k_s=0.117 \text{ W}\cdot\text{m}^{-1}\cdot\text{K}^{-1}$, the porosity $\varepsilon=0.25$ and the crystal density $\rho_s=1,430 \text{ kg}\cdot\text{m}^{-3}$ (Hanif et al., 2019). As shown in Fig. 8, the ETC of the adsorption bed varies with the amount of water absorbed by the zeolite. Since the solid phase proportion of zeolite in the adsorption bed in the experiment is between SC and FCC packing methods, the ETC of the adsorption bed should also be between the two, which is consistent with the simulation results. Moreover, the predicted ETC value of the SC packing method is closer to the experimental value than that of the FCC packing method, with a maximum error of 7.3%. The deviation between the simulated and experimental results in this work is concessional. Therefore, the SC packing method can predict the ETC of the adsorbed heat storage bed well.

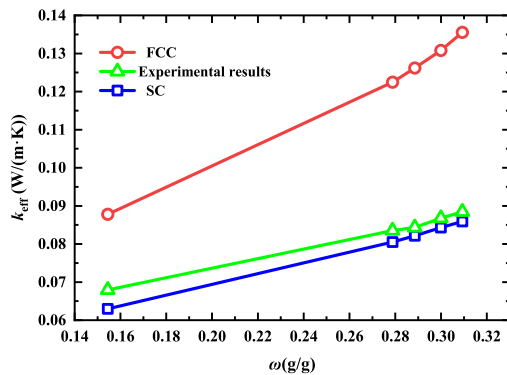


Fig. 8. Comparison of calculated ETC values of zeolite adsorption bed with results from Hanif et al. (2019).

3.4 Error analysis of simulation results

The models constructed in this paper are all based on the QSGS method and exhibit randomness. Therefore, it is necessary to analyze and compare the errors generated by model construction to ensure the stability and effectiveness of the simulation results. As depicted in Fig. 9, three numerical examples were carried out to verify the SC, FCC

and QSGS packing methods, respectively. In cases with the same structural parameters, we calculate the average of the three simulation results of ETC and compare them, with the maximum error being 0.08%. Therefore, the structural errors caused by random packing can be neglected without altering the parameters of the model construction.

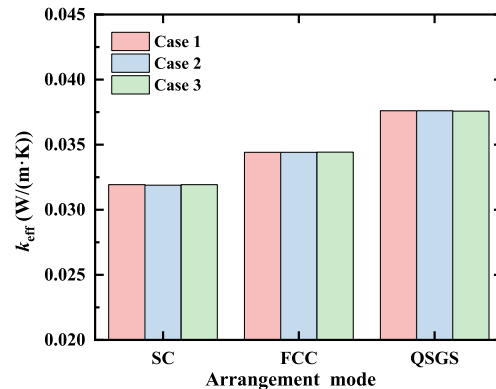


Fig. 9. Comparison of the results of three calculations.

4. Results and discussion

4.1 Effect of water absorption on the ETC of the zeolite adsorption bed

Fig. 10 illustrates the variation of the ETC of a zeolite adsorption bed at different water uptakes. The simulation results demonstrate that at a constant temperature ($t = 25^\circ\text{C}$), the ETC of the zeolite adsorption bed sharply increases with increasing water uptake. This is due to water occupying the initially porous area within the adsorption bed, progressively replacing the volume fraction of the pore phase with the adsorbate phase, and water having substantially higher heat conductivity in the pores than moist air. Moreover, as the water uptake increases from 0 to 0.32 g/g, the thermal conductivity of the FCC packing method increases by $0.0057 \text{ W}\cdot\text{m}^{-1}\cdot\text{K}^{-1}$,

while the thermal conductivity of the SC packing method only increases by $0.0038 \text{ W}\cdot\text{m}^{-1}\cdot\text{K}^{-1}$. This is because the FCC packing method has a higher volume fraction of the adsorbent phase, resulting in a larger volume fraction of the adsorbate phase for the same water uptake, which exhibits a higher thermal conductivity.

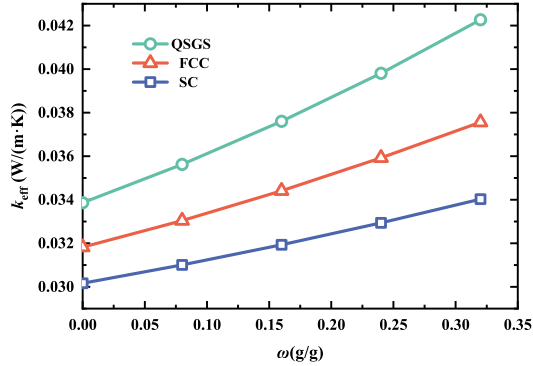


Fig. 10. Influence of water uptake on the ETC of zeolite in an adsorption bed ($t = 25^\circ\text{C}$).

4.2 Effect of temperature on the ETC of the zeolite adsorption bed

Fig. 11 illustrates the variations in ETC of the zeolite adsorption bed across different temperatures. The simulation outcomes demonstrate that, under a specific water absorption condition ($\omega = 0.16 \text{ g/g}$), the ETC of the zeolite adsorption bed exhibits an increasing trend with the elevation of temperature and demonstrates a linear relationship. This phenomenon can be attributed to the linear augmentation of the thermal conductivity of zeolite and wet air with temperature, which collectively contribute to over 95% of the volume fraction of the adsorption bed. Compared with the SC and FCC packing methods, the QSGS packing method results in a higher ETC of the adsorption bed due to its higher adsorbent phase volume fraction. It is worth noting that at $t = 85^\circ\text{C}$, the ETC of the QSGS packing adsorption bed is $0.0065 \text{ W}\cdot\text{m}^{-1}\cdot\text{K}^{-1}$ higher than the ETC of the SC packing adsorption bed.

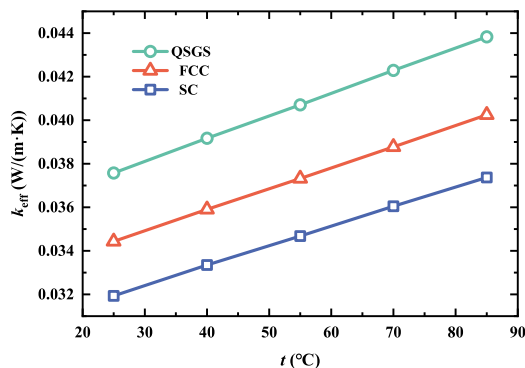


Fig. 11. Influence of temperature on the ETC of zeolite in an adsorption bed ($\omega = 0.16 \text{ g/g}$).

4.3 Effect of porosity on the ETC of the zeolite adsorption bed

At 25°C and a water absorption of 0.16 g/g , the ETC of the zeolite-filled bed is significantly influenced by the porosity of the zeolite particles, as illustrated in Fig. 12. Specifically, for the QSGS packing method, the ETC decreases from approximately 0.094 to $0.038 \text{ W}\cdot\text{m}^{-1}\cdot\text{K}^{-1}$ as the porosity escalates from 40 to 80%. Additionally, the packing method significantly influences the heat transfer dynamics, particularly in scenarios with high porosity. At a porosity of 50%, the ETC values for the adsorption beds with QSGS packing, FCC packing, and SC packing are 0.075 , 0.058 and $0.046 \text{ W}\cdot\text{m}^{-1}\cdot\text{K}^{-1}$, respectively. It is evident that the solid-phase volume fraction of the adsorption bed exerts a considerable influence on the ETC of the adsorption bed. This is fundamentally due to the thermal conductivity of zeolite being significantly higher than that of wet air.

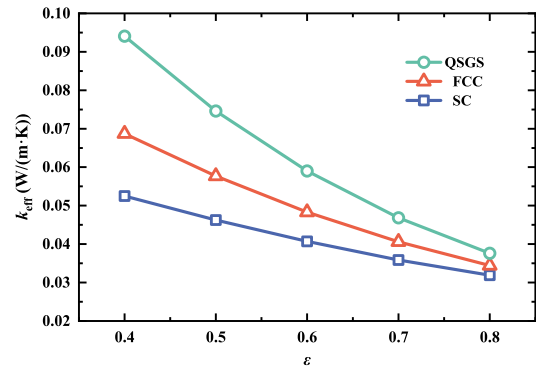


Fig. 12. Influence of porosity on the ETC of zeolite in an adsorption bed.

4.4 Effect of the contact ratio of zeolite particles on the ETC of the adsorption bed

For SC and FCC packing methods, the contact ratio of zeolite particles is a crucial factor influencing the ETC of the adsorption bed. In this study, the contact ratio is increased by increasing the particle radius. A larger contact ratio correlates with a greater solid-phase volume fraction. Fig. 13 showcases the SC packing method as an example. Compared to Fig. 13(a), Fig. 13(b) exhibits a higher contact ratio and an augmented contact area between particles, which should lead to improved heat transfer efficacy. As demonstrated in Fig. 14, for the SC packing mode, the contact ratio rises from 0 to 0.52, the ETC of the filled bed climbs from 0.032 to $0.034 \text{ W}\cdot\text{m}^{-1}\cdot\text{K}^{-1}$. For the FCC packing method, the contact ratio ascends from 0.06 to 0.45 and the ETC of the adsorption bed elevates from 0.034 to $0.037 \text{ W}\cdot\text{m}^{-1}\cdot\text{K}^{-1}$.

4.5 Effect of skeleton structure on the ETC of the zeolite adsorption bed

The c_d governs the distribution of zeolite matrix particles. As depicted in Fig. 15(a), the zeolite matrix particles are uniformly distributed when $c_d = 0.1$. Conversely, Fig. 15(b) illustrates that when $c_d = 0.001$, the distribution of zeolite

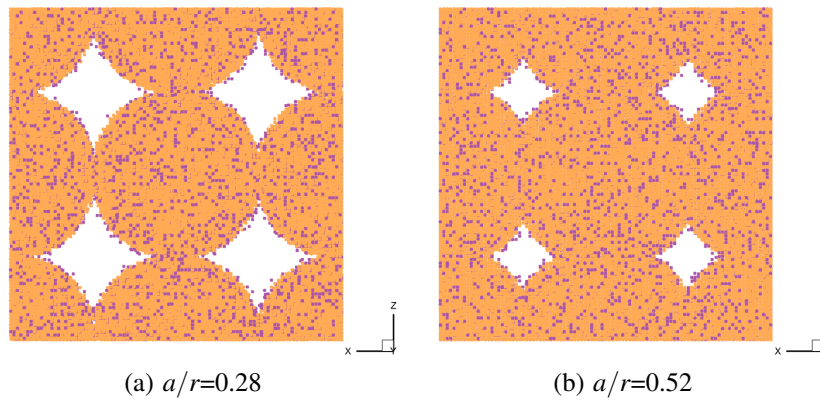


Fig. 13. Physical model of the SC packing method under different contact ratios.

matrix particles exhibits localized aggregation, resulting in the formation of large pores.

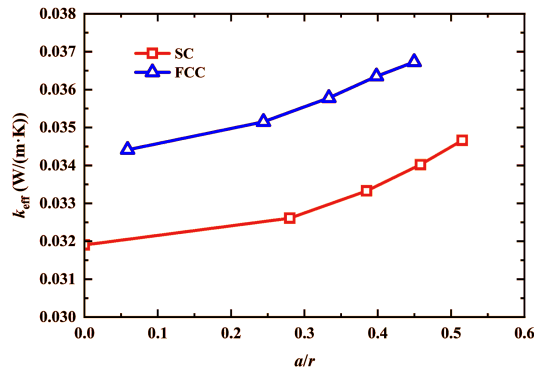


Fig. 14. Influence of contact ratio on the ETC of zeolite in an adsorption bed.

Fig. 16 presents the ETC of the adsorption bed under varying c_d conditions. It can be observed that the ETC of the adsorption bed decreases with an increase in c_d , although the effect is not pronounced. Specifically, for SC packing with a smaller solid phase volume fraction, an increase in c_d from 0.001 to 0.1 results in only a $0.0009 \text{ W}\cdot\text{m}^{-1}\cdot\text{k}^{-1}$ reduction in the ETC of the filled bed. This is due to the fixed particle packing method, which causes the distribution of the zeolite matrix particles to tend toward uniformity, thereby diminishing the impact of the c_d .

Directional growth probability D_i can regulate the anisotropy degree of zeolite matrix particles during their growth. As shown in Fig. 17(a), setting $D_{1,2,3,4} = 0.1$ ensures more substantial growth of the skeleton perpendicular to the heat conduction direction, resulting in a layered structure for the QSGS packing. Conversely, Fig. 17(b) illustrates that setting $D_{5,6} = 0.1$ promotes more substantial growth of the skeleton parallel to the heat conduction direction, leading to a strip structure in the QSGS packing.

Fig. 18(a) demonstrates the variation in the ETC of the adsorption bed with the increase of $D_{1,2,3,4}$ under the layered structure. It can be observed that the ETC of the adsorption bed gradually decreases, although the change is not pronounced.

In contrast, Fig. 18(b) depicts the change in the ETC of the adsorption bed with the increase of $D_{5,6}$, revealing a significant increase in the ETC of the adsorption bed. This phenomenon can be explained by the vertical orientation of the high and low-temperature boundaries, which leads to improved heat transfer performance of the strip structure in this particular orientation.

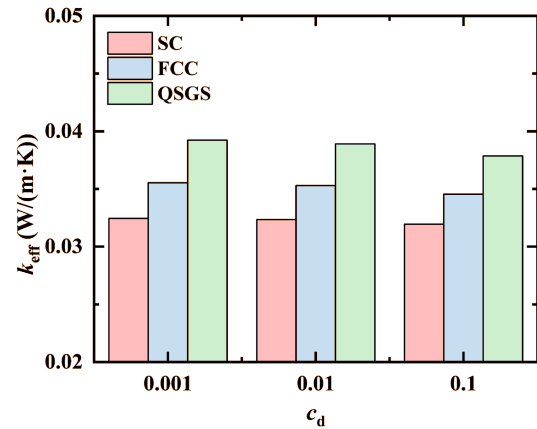


Fig. 16. Influence of c_d on the ETC of zeolite in an adsorption bed.

5. Conclusions

In this study, a novel structural algorithm, named the RPPA, was proposed for reconstructing the random adsorption structure of a zeolite adsorption bed. The ETC of the zeolite adsorption bed was calculated using the LBM. In addition, the impact of diverse parameters such as water absorption, temperature, porosity, contact ratio of zeolite particles and skeleton structure on the ETC of the zeolite adsorption bed was investigated. The results can be concisely summarized as follows:

- 1) The ETC of the zeolite adsorption bed rises with increasing water absorption. This is because the wet air in the zeolite particles' pores is gradually replaced by adsorbed water and the thermal conductivity of the water in the pores is significantly higher than that of the wet air.

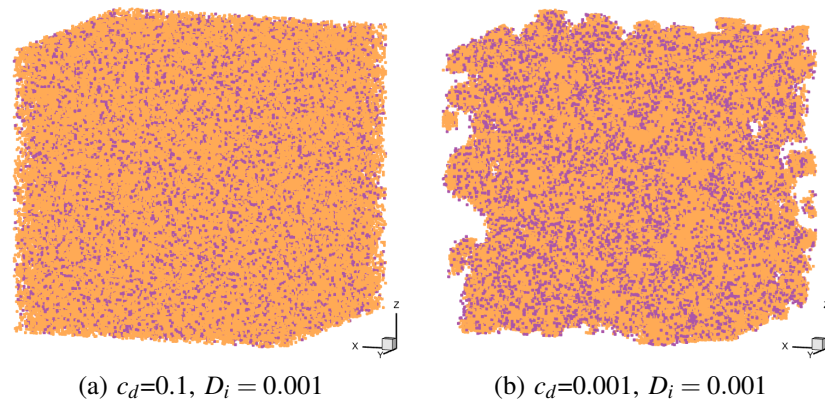


Fig. 15. Physical model of the SC packing method under different contact ratios.

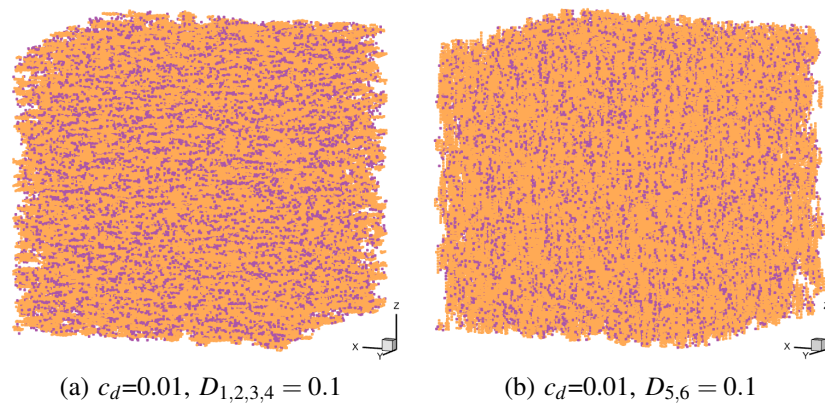


Fig. 17. QSGS packing physical model with different growth probabilities (D_i).

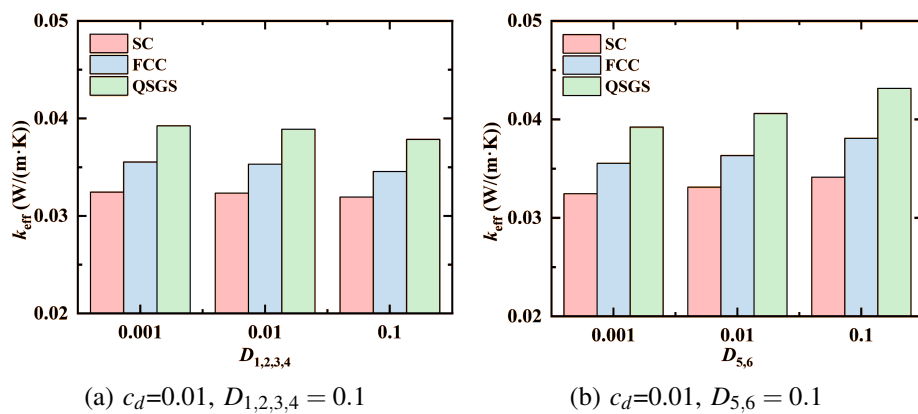


Fig. 18. Influence of D_i on the ETC of zeolite in an adsorption bed.

- 2) The ETC of the zeolite adsorption bed grows linearly with temperature under the assumption of constant water absorption. The result is caused by the zeolite and wet air's total volume component of over 95%, which increases thermal conductivity linearly with temperature.
- 3) The porosity of the zeolite particles has a significant effect on the ETC of the zeolite adsorption bed. Reducing the porosity of zeolite particles will increase the solid phase volume fraction of the material, which will improve the ETC of the adsorption bed since zeolite has a higher thermal conductivity than moist air.
- 4) By increasing the contact ratio between particles, the SC and FCC adsorption bed models, which are based on the RPPA method, can improve the thermal conductivity of the zeolite adsorption bed.
- 5) The influence of the c_d on the ETC of the zeolite adsorption bed is minimal. However, a significant enhancement in the ETC of the zeolite adsorption bed can be achieved by increasing the upward growth probability along the temperature gradient.

Acknowledgements

This work was supported by the National Natural Science Foundation of China (No. 52006243, and No. 51936001), the Natural Science Foundation of Shandong Province (No. ZR2020QE197), Qingdao Postdoctoral Application Research Project (No. qdyy20190093), and the Fundamental Research Funds for the Central Universities (No. 20CX06055A).

Conflict of interest

The authors declare no competing interest.

Open Access This article is distributed under the terms and conditions of the Creative Commons Attribution (CC BY-NC-ND) license, which permits unrestricted use, distribution, and reproduction in any medium, provided the original work is properly cited.

References

Abohamzeh, E., Frey, G. Numerical investigation of the adsorption process of zeolite/water in a thermochemical reactor for seasonal heat storage. *Energies*, 2022, 15(16): 5944.

Bon, V., Senkovska, I., Evans, J. D., et al. Insights into the water adsorption mechanism in the chemically stable zirconium-based MOF DUT-67—a prospective material for adsorption-driven heat transformations. *Journal of Materials Chemistry A*, 2019, 7(20): 12681-12690.

Chen, L., He, A., Zhao, J., et al. Pore-scale modeling of complex transport phenomena in porous media. *Progress in Energy and Combustion Science*, 2022, 88: 100968.

Chu, Z., Zhou, G., Li, R. Enhanced fractal capillary bundle model for effective thermal conductivity of composite-porous geomaterials. *International Communications in Heat and Mass Transfer*, 2020, 113: 104527.

Dawoud, B., Sohel, M. I., Freni, A., et al. On the effective thermal conductivity of wetted zeolite under the working conditions of an adsorption chiller. *Applied Thermal Engineering*, 2011, 31(14-15): 2241-2246.

Dicaire, D., Tezel, F. H. Regeneration and efficiency characterization of hybrid adsorbent for thermal energy storage of excess and solar heat. *Renewable Energy*, 2011, 36(3): 986-992.

Duan, X., Qian, Z., Tuo, Y., et al. Atomistic insights into the effect of functional groups on the adsorption of water by activated carbon for heat energy storage. *Molecules*, 2023, 29(1): 11.

Gaeini, M., Rouws, A. L., Salari, J. W. O., et al. Characterization of microencapsulated and impregnated porous host materials based on calcium chloride for thermochemical energy storage. *Applied Energy*, 2018, 212: 1165-1177.

Gao, S., Wang, S., Hu, P., et al. Performance of sorption thermal energy storage in zeolite bed reactors: Analytical solution and experiment. *Journal of Energy Storage*, 2023, 64: 107154.

Guo, B., Xu, H., Zhao, C. Lattice Boltzmann modelling on pore-scale reactive transport in exothermic reactions of solid blocks for thermochemical energy storage. *Applied Thermal Engineering*, 2022, 216: 119145.

Hanif, S., Sultan, M., Miyazaki, T. Effect of relative humidity on thermal conductivity of zeolite-based adsorbents: Theory and experiments. *Applied Thermal Engineering*, 2019, 150: 11-18.

Hu, P., Wang, S., Wang, J., et al. Scale-up of open zeolite bed reactors for sorption energy storage: Theory and experiment. *Energy and Buildings*, 2022, 264: 112077.

Hua, W., Yan, H., Zhang, X., et al. Review of salt hydrates-based thermochemical adsorption thermal storage technologies. *Journal of Energy Storage*, 2022, 56: 106158.

Igarashi, H., Uchida, H., Suzuki, M., et al. Removal of carbon monoxide from hydrogen-rich fuels by selective oxidation over platinum catalyst supported on zeolite. *Applied Catalysis A: General*, 1997, 159(1-2): 159-169.

Ito, A. Dehumidification of air by a hygroscopic liquid membrane supported on surface of a hydrophobic microporous membrane. *Journal of Membrane Science*, 2000, 175(1): 35-42.

Jänchen, J., Ackermann, D., Stach, H., et al. Studies of the water adsorption on zeolites and modified mesoporous materials for seasonal storage of solar heat. *Solar Energy*, 2004, 76(1-3): 339-344.

Kant, K., Pitchumani, R. Advances and opportunities in thermochemical heat storage systems for buildings applications. *Applied Energy*, 2022, 321: 119299.

Kant, K., Shukla, A., Smeulders, D. M., et al. Analysis and optimization of the closed-adsorption heat storage bed performance. *Journal of Energy Storage*, 2020, 32: 101896.

Li, G., Xue, B., He, X., et al. Superhydrophobic Surface-modified zeolite to regulate the migration of nonadsorbed liquid water in an Open-loop adsorption heat pump. *Applied Thermal Engineering*, 2022, 215: 118929.

Li, W., Klemeš, J. J., Wang, Q., et al. Salt hydrate-based gas-solid thermochemical energy storage: Current progress, challenges, and perspectives. *Renewable and Sustainable Energy Reviews*, 2022, 154: 111846.

Lin, Y., Yang, C., Wan, Z., et al. Lattice Boltzmann simulation

- of intraparticle diffusivity in porous pellets with macropore structure. *International Journal of Heat and Mass Transfer*, 2019, 138: 1014-1028.
- Lin, Y., Yang, C., Zhang, W., et al. Estimation of effective thermal conductivity in open-cell foam with hierarchical pore structure using lattice Boltzmann method. *Applied Thermal Engineering*, 2023, 218: 119314.
- Liu, Y., Liu, X., Lu, S., et al. Adsorption and biodegradation of sulfamethoxazole and ofloxacin on zeolite: Influence of particle diameter and redox potential. *Chemical Engineering Journal*, 2020, 384: 123346.
- Lu, J., Tang, J., Li, J., et al. The comparison of adsorption characteristics of CO₂/H₂O and N₂/H₂O on activated carbon, activated alumina, zeolite 3A and 13X. *Applied Thermal Engineering*, 2022, 213: 118746.
- Madero-Castro, R. M., Luna-Triguero, A., Sławek, A., et al. On the use of Water and Methanol with Zeolites for Heat Transfer. *ACS Sustainable Chemistry & Engineering*, 2023, 11(11): 4317-4328.
- Marín, P. E., Milian, Y., Ushak, S., et al. Lithium compounds for thermochemical energy storage: A state-of-the-art review and future trends. *Renewable and Sustainable Energy Reviews*, 2021, 149: 111381.
- Mohammed, R. H., Mesalhy, O., Elsayed, M. L., et al. Scaling analysis of heat and mass transfer processes in an adsorption packed bed. *International Journal of Thermal Sciences*, 2018, 133: 82-89.
- N'Tsoukpoe, K. E., Restuccia, G., Schmidt, T., et al. The size of sorbents in low pressure sorption or thermochemical energy storage processes. *Energy*, 2014, 77: 983-998.
- Pérez-Botella, E., Valencia, S., Rey, F. Zeolites in adsorption processes: State of the art and future prospects. *Chemical Reviews*, 2022, 122(24): 17647-17695.
- Ristić, A., Fischer, F., Hauer, A., et al. Improved performance of binder-free zeolite Y for low-temperature sorption heat storage. *Journal of Materials Chemistry A*, 2018, 6(24): 11521-11530.
- Rouhani, M., Bahrami, M. Effective thermal conductivity of packed bed adsorbents: Part 2-Theoretical model. *International Journal of Heat and Mass Transfer*, 2018, 123: 1212-1220.
- Rouhani, M., Huttema, W., Bahrami, M. Effective thermal conductivity of packed bed adsorbents: Part 1-Experimental study. *International Journal of Heat and Mass Transfer*, 2018a, 123: 1204-1211.
- Sarwar, M. K., Majumdar, P. Thermal conductivity of wet composite porous media. *Heat Recovery Systems and CHP*, 1995, 15(4): 369-381.
- Scuiller, E., Dutournié, P., Zbair, M., et al. Thermo-physical properties measurements of hygroscopic and reactive material (zeolite 13X) for open adsorptive heat storage operation. *Journal of Thermal Analysis and Calorimetry*, 2022, 147(22): 12409-12416.
- Tong, F., Jing, L., Zimmerman, R. W. An effective thermal conductivity model of geological porous media for coupled thermo-hydro-mechanical systems with multiphase flow. *International Journal of Rock Mechanics and Mining Sciences*, 2009, 46(8): 1358-1369.
- Touloumet, Q., Postole, G., Massin, L., et al. Investigation of the impact of zeolite shaping and salt deposition on the characteristics and performance of composite thermochemical heat storage systems. *Journal of Materials Chemistry A*, 2023, 11(6): 2737-2753.
- Wang, M., Pan, N. Numerical analyses of effective dielectric constant of multiphase microporous media. *Journal of Applied Physics*, 2007, 101(11).
- Wijayanta, A. T., Ooga, S., Hironaka, S., et al. Waste heat for regeneration of a packed bed of zeolite particles. *International Journal of Heat and Mass Transfer*, 2023, 203: 123798.
- Ye, H., Tao, Y. B., Wu, Z. H. Performance improvement of packed bed thermochemical heat storage by enhancing heat transfer and vapor transmission. *Applied Energy*, 2022, 326: 119946.
- Zhu, C., Qian, Z., Duan, X., et al. Investigation of water adsorption characteristics of MgCl₂ salt hydrates for thermal energy storage: Roles of hydrogen bond networks and hydration degrees. *Journal of Energy Storage*, 2024, 81: 110476.
- Zhang, S., Wang, Z. Thermodynamics behavior of phase change latent heat materials in micro-/nanoconfined spaces for thermal storage and applications. *Renewable and Sustainable Energy Reviews*, 2018, 82: 2319-2331.
- Zhu, C., Gu, Z., Xu, H., et al. The effective thermal conductivity of coated/uncoated fiber-reinforced composites with different fiber arrangements. *Energy*, 2021, 230: 120756.
- Zhu, C., Yang, W., Xu, H., et al. A general effective thermal conductivity model for composites reinforced by non-contact spherical particles. *International Journal of Thermal Sciences*, 2021a, 168: 107088.
- Zhu, C., Yu, G., Ren, X., et al. Modelling of the effective thermal conductivity of composites reinforced with fibers and particles by two-step homogenization method. *Composites Science and Technology*, 2022, 230: 109766.